Sensitivity Analysis of Multiple Scattering Theory Applied to Tree Canopies at Microwave Frequencies

Milan Kvicera, Jonathan Israel, Fernando Perez-Fontan, Pavel Pechac

Sensitivity Analysis of Multiple Scattering Theory Applied to Tree Canopies at Microwave Frequencies

Milan Kvicera, Jonathan Israel, Fernando Perez-Fontan, and Pavel Pechac

***Abstract*—A sensitivity analysis of the multiple scattering theory applied to propagation in tree canopies is presented. This analysis aims at addressing the influence of input parameters on the canopy's equivalent scattering amplitude as well as the overall coherent and incoherent scattered fields. The main input parameters of interest were identified as frequency, number densities and dielectric parameters of branches and leaves, polarization, and a canopy shape. A number of graphical results are provided enabling to identify the key parameters of corresponding radio-wave propagation models based on the multiple scattering theory.**

***Index Terms*—Multiple scattering theory, radio-wave propagation, scattering, vegetation.**

I. Introduction

THE MULTIPLE scattering theory (MST), as developed in [1]–[3], allows us to obtain the coherent and incoherent fields scattered by an ensemble of randomly oriented and positioned particles where their density is low and their sizes are smaller than their separations [4]. Alongside the radiative transfer theory [4], in the last few decades, it has been extensively used in the area of remote sensing, e.g., [5] for the case of scattering from a layer of vegetation.

In [6]–[8], the scattering characteristics for a thin dielectric cylinder representing a tree branch and a flat cylinder (disc) representing a leaf have been introduced. The scattering amplitude tensors of these individual tree canopy elements can then be utilized to obtain the equivalent scattering amplitude, to be introduced shortly, of the whole canopy.

It should be noted that the area of application for remote sensing lies mainly in the monostatic scattering case [5]. However, MST is not restricted to this case and enables arbitrary bistatic configurations, which is the case of communication and navigation scenarios in the presence of vegetation. In fact, the current version of ITU-R Rec. P.833 [9] dealing with propagation in the presence of vegetation has incorporated MST.

The applicability of MST to such scenarios has been validated in [6]–[14]. However, although several simplifying assumptions can be made as in [10] and [13], the underlying calculations depending on a number of input parameters are still very complex. As a consequence, it is not possible to address the dependence of the obtained results on the input parameters analytically in a straightforward way and, rather, a numerical approach should be applied. Although such analysis has not been published so far, it is crucial for addressing the validity range of the propagation models based on MST, such as [9] or [12]. It should be noted that performing such an analysis is very demanding from a computation-time point of view and, thus, could be of interest to a reader wanting to implement such models.

M. Kvicera and P. Pechac are with the Department of Electromagnetic Field, Faculty of Electrical Engineering, Czech Technical University in Prague, 166 27 Prague 6, Czech Republic (e-mail: kvicemil@fel.cvut.cz; pechac@fel.cvut.cz).

J. Israel is with ONERA—The French Aerospace Lab, 31055 Toulouse, France (e-mail: Jonathan.Israel@onera.fr).

F. Perez-Fontan is with the University of Vigo, 36200 Vigo, Spain (e-mail: fpfontan@tsc.uvigo.es).

II. Multiple Scattering Theory

Based on [6]–[8] and [10], we provide here the main set of equations utilized in MST. We consider a plane wave $E_i(\mathbf{r}')$ with amplitude E_0 and polarization $\hat{\mathbf{q}}$ incident in the $\hat{\mathbf{i}}$ direction on a tree canopy (Fig. 1)

$$E_i(\mathbf{r}') = \hat{\mathbf{q}} E_0 \exp\left(-jk_0\left(\hat{\mathbf{i}}\cdot\mathbf{r}'\right)\right) \tag{1}$$

where k_0 is the free-space wavenumber. The coherent field at point $\mathbf{r}'$ inside the canopy is given by

$$E_{\mathrm{coh}}^{\mathrm{in}}(\mathbf{r}') = E_i(\mathbf{r}')\exp\left\{-j\left(K-k_0\right)s_1(\mathbf{r}')\right\} \tag{2}$$

where K is the effective propagation constant and $s_1(\mathbf{r}')$ is the distance through the canopy to a point $\mathbf{r}'$ along direction $\hat{\mathbf{i}}$. Note that K is in general complex and is equal to

$$K = K' - jK'' = k_0 + \frac{2\pi}{k_0} F^{\mathrm{eq}}(\hat{\mathbf{s}},\hat{\mathbf{i}}) \tag{3}$$

where $F^{\mathrm{eq}}(\hat{\mathbf{s}},\hat{\mathbf{i}})$ represents the canopy's equivalent scattering amplitude per unit volume in the scattering direction $\hat{\mathbf{s}}$. The canopy's specific attenuation, α_c in dB/m, is then [10]

$$\alpha_c = 8.686K''. \tag{4}$$

The field $E_s(\mathbf{r})$ scattered from points $\mathbf{r}'$ inside the canopy to a point $\mathbf{r}$ outside the canopy can be written in terms of its coherent part as

$$\langle E_s(\mathbf{r})\rangle = \int_V F^{\mathrm{eq}}(\hat{\mathbf{s}},\hat{\mathbf{i}})\frac{\exp\left(-jk_0\left|\mathbf{r}-\mathbf{r}'\right|\right)}{\left|\mathbf{r}-\mathbf{r}'\right|}E_{\mathrm{coh}}^{\mathrm{in}}(\mathbf{r}')\,dV' \tag{5}$$

and incoherent part as

$$\left\langle\left|E_s(\mathbf{r})\right|^2\right\rangle = \int_V \left|V(\mathbf{r},\mathbf{r}')\right|^2\left|E_{\mathrm{coh}}^{\mathrm{in}}(\mathbf{r}')\right|^2 dV' \tag{6}$$

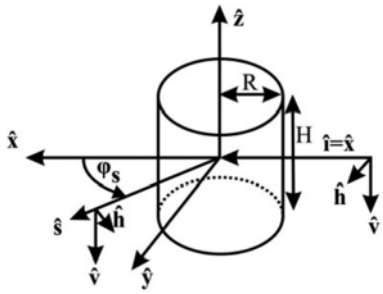

Fig. 1. Tree canopy scattering configuration.

TABLE I
SIZE OF BRANCHES AND LEAVES

Scatterer	Radius (cm)	Length/Thickness (cm)	Number Density (m^{-3})
Branch category 1	11.4	131	0.013
Branch category 2	6.0	99	0.073
Branch category 3	2.8	82	0.41
Branch category 4	0.7	54	5.1
Branch category 5	0.2	12	56
Leaf	3.7	0.02	420

where $\langle\rangle$ denotes the statistical average and $V(\mathbf{r},\mathbf{r}')$ is an operator given by

$$V(\mathbf{r},\mathbf{r}') = F^{eq}(\hat{\mathbf{s}},\hat{\mathbf{i}})\frac{\exp\left(-jk_0\left|\mathbf{r}-\mathbf{r}'\right|-j\left(K-k_0\right)s_2\left(\boldsymbol{r}'\right)\right)}{\left|\mathbf{r}-\mathbf{r}'\right|} \quad (7)$$

with $s_2(\boldsymbol{r}')$ being the distance through the canopy from a point $\mathbf{r}'$ to the point $\mathbf{r}$ along the scattering direction $\hat{\mathbf{s}}$. The coherent part is a complex electric field while the incoherent part represents a power (with no phase information).

The canopy is assumed to consist of various branch types of different sizes (divided into five categories in [9] and [10]; see Table I) and leaves with relative complex permittivity of $\epsilon_{\mathrm{b}} = 28 - 7j$ and $\epsilon_{\mathrm{l}} = 31 - 8j$, respectively. The orientations of the various types of branches and of the leaves are random and can be described by means of two rotation angles in azimuth and elevation, α and β, with respect to the tree reference coordinate frame as in [6]–[10]. Following [10], we have assumed a uniform distribution, $f_\Omega(\alpha,\beta)$, for each single branch b or leaf l. The possible range of orientation angles for the larger branches tends to be limited and centered about the vertical direction, while the smaller ones and the leaves tend to be uniformly distributed over all spatial angles.

The mean scattering amplitude is

$$\langle F^{\mathrm{b,l}}(\hat{\mathbf{s}},\hat{\mathbf{i}})\rangle = \int_0^{2\pi} d\alpha \int_0^{\pi/2} d\beta F^{b,l}(\hat{\mathbf{s}},\hat{\mathbf{i}}) f_\Omega(\alpha,\beta) \quad (8)$$

with $F^{\mathrm{b,l}}(\hat{\mathbf{s}},\hat{\mathbf{i}})$ being the scattering amplitude tensor for the branches or leaves [6]–[8]. The various types of branches and leaves are also characterized by their respective number densities $\rho_{\mathrm{b,l}}$. For the overall canopy, we can write

$$F^{\mathrm{eq}}(\hat{\mathbf{s}},\hat{\mathbf{i}}) = \sum\nolimits_{\mathrm{b}} \rho_{\mathrm{b}}\langle F^{\mathrm{b}}(\hat{\mathbf{s}},\hat{\mathbf{i}})\rangle + \rho_{\mathrm{l}}\langle F^{\mathrm{l}}(\hat{\mathbf{s}},\hat{\mathbf{i}})\rangle. \quad (9)$$

For a single branch or leaf, the mean scattering cross section can then be written as

$$\sigma^{\mathrm{b,l}}(\hat{\mathbf{s}},\hat{\mathbf{i}}) = 4\pi \int_0^{2\pi} d\alpha \int_0^{\pi/2} d\beta \left|F^{\mathrm{b,l}}(\hat{\mathbf{s}},\hat{\mathbf{i}})\right|^2 f_\Omega(\alpha,\beta) \quad (10)$$

and the equivalent scattering cross section per unit volume as

$$\sigma^{\mathrm{eq}}(\hat{\mathbf{s}},\hat{\mathbf{i}}) = 4\pi \sum\nolimits_{\mathrm{b}} \rho_{\mathrm{b}}\langle|F^{\mathrm{b}}(\hat{\mathbf{s}},\hat{\mathbf{i}})|^2\rangle + 4\pi\rho_{\mathrm{l}}\langle|F^{\mathrm{l}}(\hat{\mathbf{s}},\hat{\mathbf{i}})|^2\rangle. \quad (11)$$

In Section III, we will refer to a tree configuration studied in [10] with the same branch and leaf sizes and number densities. We may also note that following [6]–[8], the branches need to have lengths sufficiently greater than their radii, and the thickness of the leaves needs to be electrically thin.

III. SENSITIVITY ANALYSIS

From the various input parameters and their unlimited possible combinations, we have selected a representative set that enables us to provide a thorough sensitivity analysis of the behavior of MST. As mentioned above, we consider a scenario similar to the one studied in [10], i.e., a vertically polarized plane wave is incident in the $\hat{\mathbf{x}}$-direction on the canopy, and the scattering characteristics are investigated in the horizontal xy-plane for scattering angles φ_s from 0° to 180° at the distance of 50 m from the canopy center. In the analysis, (8) and (10) were evaluated by means of Monte Carlo integration. We should also note that, following [6]–[8] and [10], an infinite sum of Bessel and Hankel functions shall be utilized to obtain the scattering amplitude tensor of a single branch while [9] suggests that a maximum order of 20 is sufficient. However, even higher orders such as 50 may be required at frequencies above 10 GHz, despite the resulting increase in computation time.

A. Frequency

Keeping the dielectric parameters fixed and scanning in frequency, we obtain higher scattering amplitudes as the frequency increases for each individual canopy element. This increase is very significant, and we observe that MST calculations are strongly frequency-dependent; see for example Fig. 2, which compares the scattering amplitudes for branches of category one and leaves at 5 and 10 GHz together with the resulting overall equivalent scattering amplitudes $F^{\mathrm{eq}}(\hat{\mathbf{s}},\hat{\mathbf{i}})$.

B. Dielectric Parameters

We studied the impact of the relative permittivity ε_{r} and conductivity σ as well. It was found that at frequencies below 10 GHz, a precise characterization is not too significant; an increase/decrease of σ and ε_{r} of individual branches and leaves by 25% from their original values ($\epsilon_{\mathrm{b}} = 35 - 7j$ and $\epsilon_{\mathrm{l}} = 38.75 - 8j$, $\epsilon_{\mathrm{b}} = 21 - 7j$ and $\epsilon_{\mathrm{l}} = 23.25 - 8j$, $\epsilon_{\mathrm{b}} = 28 - 8.75j$ and $\epsilon_{\mathrm{l}} = 31 - 10j$, $\epsilon_{\mathrm{b}} = 28 - 5.25j$ and $\epsilon_{\mathrm{l}} = 31 - 6j$) did not significantly influence $F^{\mathrm{eq}}(\hat{\mathbf{s}},\hat{\mathbf{i}})$. In Fig. 3, this is shown at 2 GHz for the case of the ε_{r} increase only as the other cases had the same negligible impact.

However, at higher frequencies, the change of ε_{r} influences mainly the scattering amplitude of leaves, while the change in σ influences the resulting specific attenuation of the canopy.

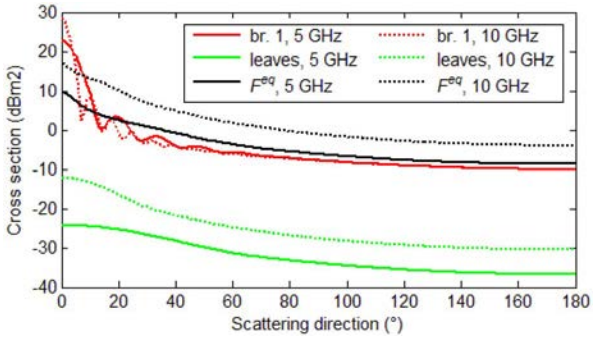

Fig. 2. Scattering amplitudes for branches of category one and leaves at the frequencies of 5 and 10 GHz together with the resulting equivalent scattering amplitude.

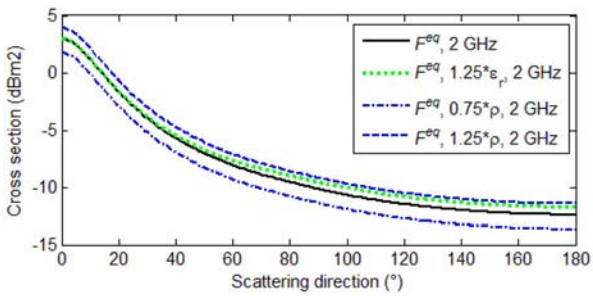

Fig. 3. Equivalent scattering amplitude per unit volume of the canopy at 2 GHz considering a 25% increase of ε_r for branches and leaves and a 25% decrease and increase of their number densities.

C. Number Densities

Number densities of branches and leaves are given in Table I [9], [10] up to a precision of three decimals. However, these values will actually vary from tree to tree, even if they belong to the same class. As the number densities influence $F^{\mathrm{eq}}(\hat{\mathbf{s}}, \hat{\mathbf{i}})$ in (9), they have a direct and significant impact on the overall coherent and incoherent fields calculated according to (5) and (6), regardless of the frequency. Fig. 3 shows $F^{\mathrm{eq}}(\hat{\mathbf{s}}, \hat{\mathbf{i}})$ for the case where all the number densities were decreased/increased by 25%. It should also be noted that at frequencies above 2 GHz, the scattering amplitude tensor of leaves increases and starts to play a major role in $F^{\mathrm{eq}}(\hat{\mathbf{s}}, \hat{\mathbf{i}})$ due to their corresponding high number density.

D. Canopy Volume Integration

Unlike in [10], the volume integration in (5) and (6) can be performed numerically, thus avoiding simplifications. Considering the coherent field calculations, the incremental volume dV' used in (5) and (6) needs to be sufficiently small to provide reliable phase information. Thus, dV' was set to be a cube of side 0.1λ, which, for large canopies and high frequencies, results in unwieldy computational demands. However, it was noticed that by increasing this side up to its 0.5λ limit, where the undersampling effects occur, the phase information in the forward scatter direction is still preserved and inaccuracy appears only towards the backscatter direction, as shown in Fig. 4. This allowed us to shorten the computation period by using dV' of side 0.2λ at 2 GHz and 0.4λ at frequencies above 10 GHz.

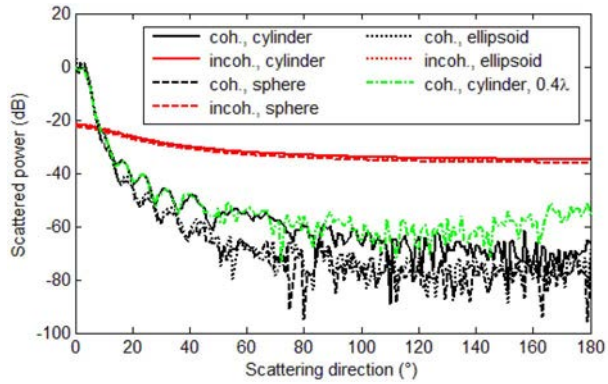

Fig. 4. Coherent and incoherent scattered fields at the frequency of 2 GHz for three different types of a tree canopy: cylindrical (radius of 5 m, height 8 m), spherical (radius of 5 m), and ellipsoidal (x and y semi-axes of 5 m, z semi-axis of 4 m). The effect of undersampling is shown by the dash-dottted line.

In this way, we were still able to well represent the coherent fields w.r.t. shadowing effects behind a tree canopy described in Section III-G. In contrast, it should be noted that the incoherent intensity calculations were not significantly influenced by utilizing the coarser canopy segmentations as they do not include the phase information.

E. Canopy Shape

References [9] and [10] suggest a cylindrical canopy. Other, more realistic shapes for some types of trees, closer for example to a sphere or an ellipsoid, can be considered.

We compared canopies approximately similar to a cylindrical one of radius 5 m and height 8 m. The comparison included a spherical canopy with radius of 5 m and an ellipsoid with x and y semi-axes of 5 m and z semi-axis of 4 m. It is obvious from Fig. 4 that the differences in the resulting fields are not very significant at 2 GHz. A similar situation was also observed at a higher frequency, 10 GHz.

In addition, no noticeable change was observed when the canopy dimensions were increased by 10%, suggesting that such precision does not play a key role.

However, it should be noted that the shadowing effects behind a tree canopy addressed in Section III-G must correspond to the canopy shape. Therefore, considering for example scenarios with inclined $\hat{\mathbf{i}}$ and $\hat{\mathbf{s}}$ directions, the canopy shape may be of greater importance than in the scenario studied in this letter.

F. Polarization

So far, only vertical polarization has been assumed. However, [6]–[8] provide equations for the horizontal polarization case as well. The corresponding mean scattering cross sections for the branches of categories one and four and leaves at 2 GHz are compared in Fig. 5 for vertical and horizontal polarizations together with the resulting $F^{\mathrm{eq}}(\hat{\mathbf{s}}, \hat{\mathbf{i}})$.

We can observe that the general levels for all branch types and the leaves remain similar when the polarization is switched, especially in the forward scatter direction.

Furthermore, the specific attenuation determined from the imaginary part of K by (4) was slightly lower (0.81 dB/m) than for the vertical polarization case (0.97 dB/m).

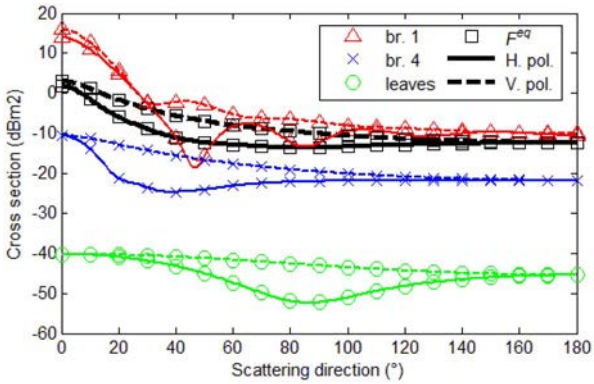

Fig. 5. Mean scattering cross sections for the leaves and branches of categories one and four at the frequency of 2 GHz for the horizontal and vertical polarizations.

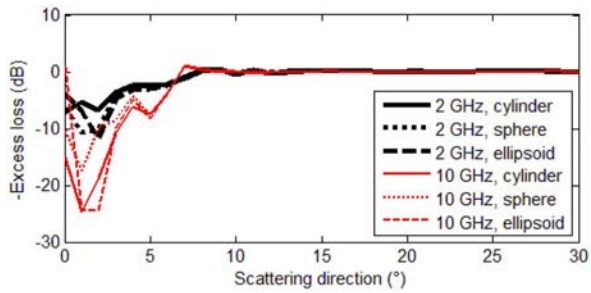

Fig. 6. Shadowing behind the canopy caused by the coherently scattered field at the frequencies of 2 and 10 GHz for the three different canopy shapes with dimensions as in Fig. 4.

G. Shadowing Effects

When added to the direct field, the coherent scattered field provides a diffraction pattern in the shadow region behind the canopy [15]. For this case, the shape of the canopy may be of importance as, in general, mainly the contributions above and below the canopy are different for spherical or cylindrical shapes. Fig. 6 shows the differences obtained at 2 and 10 GHz for cylindrical, spherical, and ellipsoidal canopies with the same dimensions as in Section III-E. Here, we can observe an overall similar trend with slightly different diffraction patterns depending on the canopy shape. The absolute values correspond to the obtained specific attenuation ($\alpha_{c,2\mathrm{GHz}} = 0.97$ dB/m, $\alpha_{c,10\mathrm{GHz}} = 2.14$ dB/m) multiplied by the propagation distance through the canopy, which is about 10 m. The geometric shadow region behind the canopy is about 6° wide, which is in good agreement with the pattern in Fig. 6.

IV. Summary

The results enabling to address the validity of corresponding propagation models based on the multiple scattering theory were presented. We have shown that apart from polarization, there are two other main input parameters of interest: frequency and number densities of branches and leaves. Although the frequency dependence can be considered to be self-explanatory, the direct influence of the number densities, often required to a precision of up to three decimals, may not be that evident. However, it was this parameter that determined the dominant role of the leaves throughout the presented analysis. Although one selected scenario was studied, the findings have a general applicability as they are based on the principal MST equations.

References

[1] L. L. Foldy, "The multiple scattering of waves. I. General theory of isotropic scattering by randomly distributed scatterers," *Phys. Rev.*, vol. 67, no. 3/4, pp. 107–119, Feb. 1945.

[2] M. Lax, "Multiple scattering of waves," *Rev. Mod. Phys.*, vol. 23, no. 4, pp. 287–310, Oct. 1951.

[3] V. Twersky, "Multiple scattering of electromagnetic waves by arbitrary configurations," *J. Math. Phys.*, vol. 8, no. 3, pp. 589–610, Mar. 1967.

[4] A. Ishimaru, *Wave Propagation and Scattering in Random Media*. New York, NY, USA: Wiley-IEEE Press, 1999.

[5] F. T. Ulaby and D. Long, *Microwave Radar and Radiometric Remote Sensing*. Ann Arbor, MI, USA: Univ. Michigan Press, 2014.

[6] M. A. Karam and A. K. Fung, "Electromagnetic scattering from a layer of finite length, randomly oriented, dielectric, circular cylinders over a rough interface with application to vegetation," *Int. J. Remote Sensing*, vol. 9, no. 6, pp. 1109–1134, 1988.

[7] M. A. Karam, A. K. Fung, and Y. M. M. Antar, "Electromagnetic wave scattering from some vegetation samples," *IEEE Trans. Geosci. Remote Sens.*, vol. 26, no. 6, pp. 799–808, Nov. 1988.

[8] M. A. Karam and A. K. Fung, "Leaf-shape effects in electromagnetic wave scattering from vegetation," *IEEE Trans. Geosci. Remote Sens.*, vol. 27, no. 6, pp. 687–697, Nov. 1989.

[9] ITU, Geneva, Switzerland, "Attenuation in vegetation," ITU-R Rec. P.833-8, 2013.

[10] Y. L. C. de Jong and M. H. A. J. Herben, "A tree-scattering model for improved propagation prediction in urban microcells," *IEEE Trans. Veh. Technol.*, vol. 53, no. 2, pp. 503–513, Mar. 2004.

[11] M. Cheffena and F. Perez Fontán, "Land mobile satellite channel simulator along roadside trees," *IEEE Antennas Wireless Propag. Lett.*, vol. 9, pp. 748–751, 2010.

[12] J. Israel and A. Pajot, "Fading and scattering due to trees in L to Ka band propagation simulations," in *Proc. 9th EuCAP*, Lisbon, Portugal, Apr. 2015, pp. 1–5.

[13] S. A. Torrico, H. L. Bertoni, and R. H. Lang, "Modeling tree effects on path loss in a residential environment," *IEEE Trans. Antennas Propag.*, vol. 46, no. 6, pp. 872–880, Jun. 1998.

[14] K. L. Chee, S. A. Torrico, and T. Kurner, "Radiowave propagation prediction in vegetated residential environments," *IEEE Trans. Veh. Technol.*, vol. 62, no. 2, pp. 486–499, Feb. 2013.

[15] Y. L. C. de Jong, "Measurement and modeling of radiowave propagation in urban microcells," Ph.D. dissertation, T.U. Eindhoven, Eindhoven, The Netherlands, 2001.